British Journal of Pharmacology (2005) 144, 265–274
www.nature.com/bjp

TNF regulates leukocyte–endothelial cell interactions and microvascular dysfunction during immune complex-mediated inflammation

[1]M. Ursula Norman, [1]Karyn J. Lister, [1]Yuan H. Yang, [2]Andrew Issekutz & *,[1]Michael J. Hickey

[1]Centre for Inflammatory Diseases, Monash University Department of Medicine, Monash Medical Centre, 246 Clayton Road, Clayton, Vic., 3168, Australia and [2]Departments of Pediatrics, Microbiology-Immunology and Pathology, Dalhousie University, Halifax, NS, Canada

1 The aim of this study was to assess directly the role of TNF in immune complex-induced leukocyte–endothelial cell interactions and microvascular dysfunction.

2 Intravital microscopy was used to examine immune complex-induced leukocyte rolling, adhesion and emigration and microvascular permeability in cremasteric postcapillary venules in wild-type and $TNF^{-/-}$ mice. The reverse passive Arthus (RPA) reaction was used to localize immune complex formation to the cremaster muscle.

3 In wild-type mice, immune complex deposition induced a reduction in leukocyte rolling velocity and increases in leukocyte adhesion and emigration. In $TNF^{-/-}$ mice, the immune complex-induced reduction in leukocyte rolling velocity was significantly attenuated, and leukocyte adhesion and emigration were also significantly reduced relative to responses in wild-type mice.

4 The alterations in $TNF^{-/-}$ mice were associated with decreased expression of endothelial P-selectin and VCAM-1, and an absence of E-selectin-dependent rolling normally seen in wild-type mice at the peak of the response. In addition, the level of immune complex-induced microvascular permeability was attenuated in $TNF^{-/-}$ mice.

5 These findings demonstrate that in immune complex-induced inflammation, TNF promotes leukocyte rolling and adhesive interactions, and entry of leukocytes into sites of immune complex deposition, in part *via* the increased expression and/or function of endothelial P-selectin, E-selectin and VCAM-1. In addition, this increase in leukocyte recruitment mediated by TNF correlates directly with an increase in microvascular injury.
British Journal of Pharmacology (2005) **144,** 265–274. doi:10.1038/sj.bjp.0706081
Published online 10 January 2005

Keywords: Selectin; rolling; adhesion; VCAM-1; cytokine; permeability

Abbreviations: ICAM-1, intercellular adhesion molecule-1; KLH, keyhole limpet hemocyanin; OVA, ovalbumin; RPA, reverse passive Arthus; VCAM-1, vascular cell adhesion molecule-1

Introduction

Leukocyte recruitment to sites of inflammation is mediated by a precise sequence of interactions between circulating leukocytes and endothelial cells, whereby leukocytes initially tether and roll along the endothelial surface, then subsequently adhere to the endothelium and emigrate out of the vasculature (Springer, 1994). In many types of inflammation, it has been shown that each of these sequential interactions is mediated by specific groups of adhesion molecules, with the selectins (P-, E- and L-) being critical in mediating rolling, and leukocyte integrins mediating adhesion *via* interaction with counter receptors on endothelial cells (Springer, 1994; Muller, 2002). A host of inflammatory mediators have been identified which are capable of inducing these interactions. One such mediator, the proinflammatory cytokine TNF, has been shown to promote leukocyte–endothelial interactions *in vitro* and *in vivo* (Abbassi *et al*., 1993; Luscinskas *et al*., 1995; Kunkel & Ley, 1996; Hickey *et al*., 1997). The *in vivo* application of exogenous TNF induces a characteristic reduction in the velocity of leukocyte rolling in postcapillary venules, and a corresponding increase in leukocyte firm adhesion and emigration into tissue (Kunkel & Ley, 1996; McCafferty *et al*., 2000; Thorlacius *et al*., 2000; Thompson *et al*., 2001). This response is associated with increased expression of the endothelial adhesion molecules P-selectin, E-selectin, vascular cell adhesion molecule-1 (VCAM-1) and intercellular adhesion molecule-1 (ICAM-1) (Mulligan *et al*., 1993; Henninger *et al*., 1997; Jung & Ley, 1997). However, it remains unclear whether the effects of TNF applied exogenously, at doses selected to generate high levels of leukocyte interactions, mimic the effects of TNF released endogenously during inflammatory responses.

One type of response in which TNF may promote leukocyte–endothelial cell interactions is immune complex-induced inflammation. Immune complexes are potent proinflammatory mediators that are believed to be major contributors to the effector phase of immunologic diseases such as systemic lupus erythematosus and rheumatoid arthritis

*Author for correspondence;
E-mail: michael.hickey@med.monash.edu.au
Published online 10 January 2005

(Firestein, 2003; Mok & Lau, 2003). There is a growing body of evidence that TNF plays an important role in the development of immune complex-induced responses. Expression of TNF has been demonstrated during immune complex-induced inflammation (Warren *et al*., 1989; Mulligan & Ward, 1992). Moreover, blockade of TNF, or the absence of TNF receptors, results in a significant reduction in immune complex-induced tissue injury in some, but not all, tissues (Warren, 1991; Mulligan & Ward, 1992; Brito *et al*., 1999). Indirect assessments such as histological assessment or measurement of tissue myeloperoxidase, as an index of leukocyte accumulation, have demonstrated that TNF also contributes to immune complex-induced leukocyte recruitment and microvascular dysfunction (Mulligan & Ward, 1992; Brito *et al*., 1999). However, the precise role of TNF in regulating the requisite rolling and adhesive interactions of leukocytes within the microvasculature during an immune complex-induced response has not been investigated.

In the lung, blockade of TNF has been shown to result in reduced ICAM-1 expression and a corresponding reduction in leukocyte entry following immune complex challenge (Mulligan *et al*., 1993). However, in recent investigations of the molecular requirements for immune complex-induced rolling and adhesion in postcapillary venules of the cremaster muscle, we have shown that P-selectin, E-selectin and VCAM-1 are required for these interactions (Norman *et al*., 2003). The role of TNF in promoting expression of these adhesion molecules during immune complex-induced injury remains unclear. Therefore, the aim of the present study was to examine this issue using intravital microscopy to visualize the microvasculature directly during an immune complex-induced response. The well-characterized reverse passive Arthus (RPA) response was used as a model of immune complex-induced leukocyte recruitment in the cremaster muscle. To elucidate the role of TNF, responses in wild-type mice were compared with those in mice genetically deficient in this cytokine. These experiments revealed that TNF plays a role in each step of the leukocyte recruitment cascade during the immune complex-induced response.

Methods

Animals

Wild-type (C57BL/6) mice were bred in-house at Monash University or purchased from Walter & Eliza Hall Institute, Melbourne, Australia, and housed in conventional conditions. Mice genetically deficient in TNF ($TNF^{-/-}$) (Korner *et al*., 1997) on a C57BL/6 background were generously supplied by Drs Jonathan Sedgwick and Nick Pearce (Centenary Institute, Sydney, Australia) and housed in specific pathogen-free conditions. All experimental procedures involving animals were approved by the Monash University Animal Ethics Committee.

Antibodies

The antibodies used in this study were: polyclonal anti-ovalbumin antibody (Sigma Chemical CO., St Louis, MO, U.S.A.); RB40.34, a monoclonal antibody (mAb) against murine P-selectin (BD Biosciences, San Diego, CA, U.S.A.); RME-1, a mAb against rat and mouse E-selectin; RMP-1, a mAb against rat and mouse P-selectin (RME-1 and RMP-1 were produced in the laboratory of A. Issekutz); 6C7.1, a mAb against murine VCAM-1 (hybridoma provided by Drs Dietmar Vestweber and Britta Engelhardt, Max Planck Institut, Meunster, Germany); and A110-2 (IgG2) (BD Biosciences), rat anti-keyhole limpet hemocyanin (KLH) (BD Biosciences), which was used as a control mAb in adhesion molecule expression experiments.

Reverse passive arthus reaction in the cremaster muscle

As previously described, the RPA model of immune complex-induced leukocyte recruitment was induced by the intravenous (i.v.) injection of 500 μg of ovalbumin (OVA; Sigma Chemical CO., St Louis, MO, U.S.A., 100 μl of 5 mg ml^{-1}, in sterile saline), followed by the intrascrotal injection of 100 μg of polyclonal anti-ovalbumin antibody in 200 μl sterile saline (Norman *et al*., 2003). Responses in the left cremaster muscle were then assessed 4 h after induction of the RPA response.

Intravital microscopy

Mice were anesthetised with ketamine hydrochloride (200 mg kg^{-1}; Pfizer, West Ryde, New South Wales, Australia) and xylazine (10 mg kg^{-1}; Troy Laboratories, Smithfield, NSW, Australia) by intraperitoneal (i.p.) injection. The left jugular vein was cannulated to administer additional anesthetic and antibody treatments. Animals were maintained at 37°C on a thermocontrolled heating pad. The cremaster muscle was dissected free of connective tissues and exteriorized onto an optically clear viewing pedestal. The muscle was cauterized longitudinally and held flat against the optical window by attaching silk sutures to the corners of the tissue. The tissue was kept warm and moist throughout the experiments by superfusion of warmed bicarbonate-buffered saline (pH 7.4) and covered with a coverslip, held in place with vacuum grease.

The cremasteric microcirculation was visualized using an intravital microscope (Axioplan 2 Imaging; Carl Zeiss, Australia) with a $\times 20$ objective lens (LD Achroplan $20\times/0.40$ NA, Carl Zeiss, Australia) and a $\times 10$ eyepiece. A color video camera (Sony SSC-DC50AP, Carl Zeiss, Australia) was used to project the images onto a calibrated monitor (Sony PVM20N5E) and the images were recorded for playback analysis using a videocassette recorder (Panasonic NV-HS950, Klapp Electronics, Prahran, Vic., Australia). Two to four venules (25–40 μm in diameter) were selected in each experiment and to minimize variability the same section of each venule was observed throughout the experiment. Data from individual vessels were averaged for each mouse, then group means were generated from these averages. n is used to denote the number of mice examined. Venular diameter (D_V) and the number of rolling and adherent leukocytes were determined off-line during video playback analysis. Rolling leukocytes were defined as those cells moving at a velocity less than that of erythrocytes within a given vessel. Leukocyte rolling velocity was determined by measuring the time required for a leukocyte to roll along a 100 μm length of venule, and quantitated for 20 leukocytes at each time interval. Leukocyte rolling flux was defined as the number of rolling cells moving past a fixed point on the venular wall per minute, averaged over 2 min. Leukocytes were considered to be adherent to the

venular endothelium if they remained stationary for 30 s or longer within a given 100 μm vessel segment. Leukocyte emigration was defined as the number of extravascular leukocytes visible per microscopic ($\times$ 20) video field centered on a postcapillary venule, and was determined by averaging data derived from 6–10 fields 5 h post-RPA. Centerline red blood cell velocity (V_{RBC}) was measured on-line using an optical Doppler velocimeter (Microcirculation Research Institute; Texas A&M University, College Station, TX, U.S.A.) and mean red blood cell velocity (V_{MEAN}) was determined as $V_{RBC}/1.6$. Venular wall shear rate (γ) was calculated based on the Newtonian definition: $\gamma = 8\ (V_{MEAN}/D_V)$.

The degree of macromolecular leakage from cremasteric venules was assessed using a modification of a previously published technique (Hickey *et al*., 1998). Briefly, FITC-labelled 70 kDa-dextran (Sigma-Aldrich, Castle Hill, New South Wales, Australia, 125 $\mu g\,g^{-1}$, 5% in saline) was injected i.v. at the start of the experiment, and FITC-derived fluorescence (excitation wavelength – 450–490 nm, emission wavelength – 515 nm, Carl Zeiss filter set 09) within the cremasteric microvasculature was detected using a silicon intensified target camera (Dage-MTI VE-1000; Sci Tech Pty, Ltd, Preston South, Vic., Australia) at predefined gain and black level settings. Images were captured directly from the camera (*PC2-Vision* capture board, *Coreco Imaging*, Billerica, MA, U.S.A.) and *Scion Image* image analysis software (Scion Corp., Frederick, MD, U.S.A.) used to determine the intensity of FITC-derived fluorescence within the lumen of the venule and in adjacent perivascular tissue. Background was defined as the fluorescence intensity prior to FITC-dextran administration. Vascular permeability was determined according to the ratio (mean interstitial intensity−background)/(mean venular intensity−background), and expressed as a percentage.

Experimental protocol

It has been previously shown that peak levels of leukocyte/endothelial interactions occur 4 h after induction of the RPA response (Norman *et al*., 2003). Therefore, initial experiments examined the RPA response after 4 h in wild-type and $TNF^{-/-}$ animals. To determine the role of endothelial adhesion molecules in $TNF^{-/-}$mice, additional mice underwent the RPA response and were subsequently treated with a function-blocking P-selectin antibody (RB40.34, 20 μg per mouse) shortly after the 4-h time point. For comparison, wild-type mice were treated with either RB40.34 or an E-selectin blocking antibody (RME-1, 100 μg per mouse). RME-1 has previously been shown to increase leukocyte rolling velocity in cremasteric venules following LPS treatment, similar to the effect of alternative anti-E-selectin antibodies (Hickey *et al*., 1998). The effects of these treatments on leukocyte rolling parameters were assessed.

In order to test the role of TNF specifically in adhesion during the RPA response, $TNF^{-/-}$ mice were allowed to undergo the RPA response without intervention for 4 h. A recording of the microvasculature was made at 4 h and then the muscle was superfused with TNF (165 $ng\,ml^{-1}$ in superfusion buffer). The ability of this treatment to affect adhesion acutely was determined by examination of the vasculature 15 and 30 min later. To assess the role of TNF in mediating increased vascular permeability, vascular permeability was compared in wild-type and $TNF^{-/-}$ mice 4.5 h after the initiation of the RPA response. In addition, $TNF^{-/-}$ mice were treated with TNF (50 ng, intrascrotal) at the initiation of the RPA response to determine if replacing the TNF could restore the permeability response in $TNF^{-/-}$ mice.

Quantification of TNF mRNA via *real-time PCR*

Real time PCR was used to measure TNF mRNA in the cremaster muscle. RNA was extracted from tissue samples *via* homogenization in TRIzol (Gibco BRL, Grand Island, NY, U.S.A.). One μg of the total RNA was reverse transcribed using Superscript II reverse transcriptase (Gibco BRL) and oligo-(dT) (12–15). PCR amplification was performed on a LightCycler (Roche Diagnostics, Castle Hill, NSW, Australia) using SYBR Green I, as previously described (Drummond *et al*., 2000). Murine TNF and β-actin PCR products were employed as assay standards. Amplification (40 cycles) was carried out in a total volume of 10 μl containing 1 μl dNTP mix, *Taq*, SYBR Green I dye and the following primers at 3 pM – TNF (5′-CCTCTTCTCATTCCTGCTT-3′ and 5′-CACTTGGTGGTTTGCTACGA-3′) and β-actin (5′-TGTCCCTGTATGCCTCTGGT-3′ and 5′-GATGTCACGCACGATTTCC-3′). Melting curve analysis and agarose gel electrophoresis were performed at the end of each PCR reaction. Quantification of the ratio of TNF mRNA to β-actin mRNA was performed by determining the threshold cycle (CT) and using a standard curve to determine the starting RNA concentration for each gene. Calculation of CTs, preparation of standard curves and determination of starting concentrations for samples were performed by the LightCycler computer software.

Quantification of endothelial adhesion molecule expression

Endothelial expression of P-selectin and VCAM-1 was quantified using a dual antibody labelling method described previously (Norman *et al*., 2003). Briefly, anti-P-selectin antibody (RMP-1) and anti-VCAM-1 antibody (6C7.1) were conjugated to Alexa Fluor 488 (Molecular Probes, Eugene, OR, U.S.A.). As a control antibody, anti-KLH was conjugated with Alexa Fluor 594. Tissue distribution of antibodies conjugated to Alexa-488 was determined by epi-illumination at 450–490 nm, with a 515 nm emission filter. Alexa-594-associated fluorescence was detected by epi-illumination at 530–585 nm excitation filter, with a 615 nm emission filter (Carl Zeiss filter set 00). Images were visualized using a SIT video camera (Dage-MTI VE-1000) on predefined gain and black level settings, and recorded for subsequent playback analysis using a videocassette recorder.

After the desired experimental protocol, mice were anesthetised and the right carotid artery and the left jugular vein were cannulated. To detect expression of P-selectin or VCAM-1, mice received 100 μg of RMP-$1^{ALEXA\ 488}$ or 90 μg of 6C7.$1^{ALEXA\ 488}$ (doses previously determined to saturate available receptors) and 20 μg of anti-$KLH^{ALEXA\ 594}$ intravenously. Antibodies were allowed to circulate for 5 min, and then the mouse was exsanguinated *via* the carotid artery cannula with simultaneous perfusion of bicarbonate-buffered saline *via* the jugular vein. An additional 15 ml of buffer was subsequently backflushed through the carotid artery after severing the abdominal vena cava. The left cremaster was

prepared for microscopy and the microcirculation was visualized to detect P-selectin or VCAM-1 expression. Given that tissue exteriorization does not occur until after the staining procedure is completed, this excludes any possible contribution of exteriorization-induced adhesion molecule upregulation.

The vasculature was first assessed for nonspecific (anti-$KLH^{ALEXA\ 594}$) labelling. Vessels containing detectable Alexa-594-associated fluorescence were deemed to have been inadequately exsanguinated and were excluded from analysis. In most experiments, this applied to a maximum of 1–2 vessels. Analyses were performed on captured video frames using *Scion Image* analysis software. Two measurements of adhesion molecule expression were made. Firstly, the length of vessel containing specific ($RMP\text{-}1^{ALEXA\ 488}$ or $6C7.1^{ALEXA\ 488}$) labelling was determined for 15–30 sequential $\times 10$ (Achroplan 10X/0.25 NA, Carl Zeiss) fields (mm mm^2 tissue $area^{-1}$). Secondly, the intensity of staining in individual vessels was determined for 15–30 $\times 20$ (LD Achroplan $20\times/0.40$ NA, Carl Zeiss) fields. The intensity of Alexa-488-derived fluorescence associated with the vascular wall, and that in the avascular surrounding tissue were measured. The intensity of extravascular fluorescence was subtracted from that present in the vessel wall, and the resultant intensity readings were averaged over the length of the vascular wall assessed. Final data were calculated as the product of the average intensity multiplied by the length of positive vessel.

Circulating leukocyte counts and flow cytometry

At the end of each experiment, whole blood was drawn *via* cardiac puncture. Total leukocyte counts were performed using a Neubauer hemocytometer (U-Lab, Eltham, Australia). Circulating leukocytes were identified in whole blood using flow cytometry. The mAbs used were as follows (purchased from BD Biosciences, San Diego, CA, U.S.A., unless otherwise stated): APC-conjugated 30-F11 (anti-CD45); PE-conjugated 17A2 (anti-CD3); PE-conjugated GK1.5 (anti-CD4); APC-conjugated 53–6.7 (anti-CD8a); PE-conjugated RB6-8C5 (anti-Ly-6G/Gr-1); FITC-conjugated RA3-6B2 (anti-B220); and KT3 (anti-CD3) and M1/70 (anti-Mac-1), both purified from hybridoma supernatant, and conjugated in-house to Alexa-488. Briefly, 100 μl aliquots of blood were incubated with appropriate mixtures of mAbs for 25 min. Samples underwent subsequent erythrocyte lysis and paraformaldehyde fixation using a Q-Prep Workstation (Beckman Coulter, Miami, FL, U.S.A.) and were analyzed using a MoFlo flow cytometer (Cytomation, Fort Collins, CO, U.S.A.). $CD45^+$ leukocytes were subsequently classified as follows: granulocytes – $Gr\text{-}1^{hi}/M1/70^+$; monocyte lineage cells – $Gr\text{-}1^{Int}/M1/70^+$; T cells – $CD3^+/B220^-$; and B cells – $B220^+/CD3^-$ in accordance with previous observations in mice.

Statistical analysis

All data are displayed as mean $\pm$ s.e.m. For comparisons involving only two groups, Student's *t*-tests were used. Paired analysis was used for comparison between before and after antibody treatment. A value of $P<0.05$ was deemed significant.

Results

$TNF^{-/-}$ mice have previously been shown to have increased circulating leukocyte counts. Given the potential for this to affect leukocyte trafficking parameters, we first assessed the circulating leukocyte populations in $TNF^{-/-}$ mice. In accordance with previous observations (Korner *et al*., 1997), circulating leukocyte counts were significantly elevated in $TNF^{-/-}$ mice relative to wild-type mice (Table 1). Analysis of the composition of the circulating leukocytes revealed that the percentages of granulocytes, monocyte lineage cells, T cells and B cells, as well as the ratio of $CD4^+$ to $CD8^+$ T cells in the blood, did not differ between the strains (data not shown).

We next compared the microvasculatures of wild-type and $TNF^{-/-}$ mice in the absence of exogenous inflammatory stimulation. In untreated animals, venular diameters and microvascular shear rates did not differ significantly between wild-type and $TNF^{-/-}$ mice (Table 1). Similarly, leukocyte rolling velocity, rolling flux, adhesion and emigration did not differ in untreated mice (Figure 1).

Immune complex-induced inflammation in TNF-deficient mice

Previously we have observed that the RPA model of immune complex-induced inflammation causes a reduction in leukocyte rolling velocity, as well as significant increases in adhesion and emigration within 4 h (Norman *et al*., 2003). To determine the role of TNF in regulating these interactions, we compared RPA-induced leukocyte–endothelial cell interactions in wild-type and $TNF^{-/-}$ mice. Following RPA treatment, venular diameter and shear rate were not significantly different from RPA-treated wild-type mice (Table 1). Similarly, following RPA treatment leukocyte rolling flux did not differ significantly between the strains (wild-type – 43.7 ± 7.7 vs $TNF^{-/-}$ – 68.9 ± 11.9 cells min^{-1}). In contrast, leukocyte rolling velocity

Table 1 Venular diameter, microvascular shear rates and number of circulating leukocytes in wild-type and $TNF^{-/-}$ mice, in the absence of treatment, or 4 h after initiation of RPA response

	Untreated wild-type	*Wild-type RPA 4 h*	*Untreated $TNF^{-/-}$*	*$TNF^{-/-}$ RPA 4 h*
Venular diameter (μm)	30.1 ± 1.4	32.2 ± 0.8	34.5 ± 1.9	25.7 ± 0.9
Shear rate (s^{-1})	449 ± 34	383 ± 38	463 ± 26	462 ± 29
Circulating leukocytes (cells $\times 10^6$ ml^{-1})	2.7 ± 0.5	3.1 ± 0.7	9.1 ± 0.9^a	7.1 ± 1.3^b
(*n*)	(6)	(6)	(6)	(6)

Data are shown as mean $\pm$ s.e.m. *n* denotes number of mice examined.
[a]Represents $P<0.05$ relative to untreated wild-type mice.
[b]Denotes $P<0.05$ relative to RPA-treated wild-type mice.

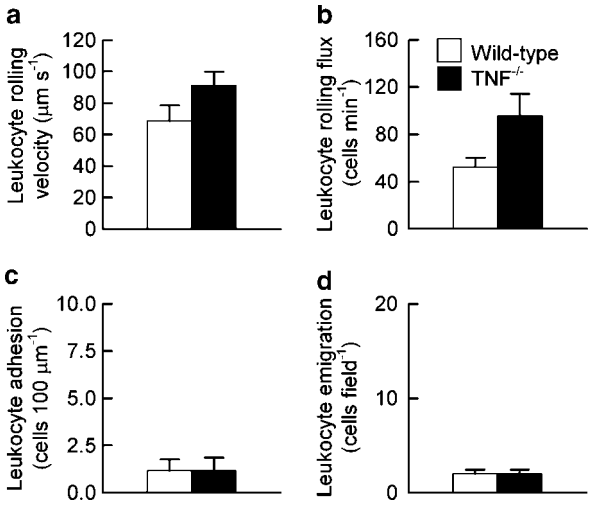

Figure 1 Leukocyte rolling velocity (a), rolling flux (b), adhesion (c) and emigration (d) in cremasteric postcapillary venules of untreated wild-type and TNF$^{-/-}$ mice, 30 min after exteriorization. Data are shown as mean ± s.e.m. of 6–7 animals.

during the RPA response was altered in mice lacking TNF. The normal reduction in leukocyte rolling velocity seen in wild-type mice (Norman *et al*., 2003) was significantly attenuated in TNF$^{-/-}$ mice to the extent that the mean velocity in TNF$^{-/-}$ mice was greater than double that observed in wild-type mice 4 and 4.5 h after RPA initiation (Figure 2a). Similarly, the number of adherent leukocytes was significantly decreased in TNF$^{-/-}$ mice compared to wild-type mice 4 and 4.5 h after RPA induction (Figure 2b). Finally, these reductions in leukocyte-endothelial interactions in TNF$^{-/-}$ mice were associated with a significant reduction (>75%) in leukocyte entry into tissues, as demonstrated by the assessment of emigration (Figure 2c). These observations indicate that each of the steps in the leukocyte recruitment cascade during immune complex-induced inflammation is reduced in TNF$^{-/-}$ mice.

Expression of TNF mRNA in wild-type mice

We next used real-time PCR to investigate alterations in the expression of TNF mRNA in the cremaster muscle induced by the RPA protocol. RPA treatment induced a six-fold increase in TNF mRNA expression (Figure 3).

Differential endothelial selectin usage in TNF$^{-/-}$ mice

We have previously observed that leukocyte rolling in wild-type mice 4 h after RPA initiation is mediated by both P- and E-selectin (Norman *et al*., 2003). Acute administration of anti-P-selectin mAb reduces rolling flux by approximately 75% in RPA-treated wild-type mice, with the residual rolling being E-selectin-dependent. In contrast, in the present experiments leukocyte rolling in RPA-treated TNF$^{-/-}$ mice was almost entirely eliminated (>95% inhibition) by acute P-selectin blockade (Figure 4), an effect not seen after administration of an isotype control antibody. These findings indicate that the functional role of E-selectin in the wild-type RPA response is dependent on the presence of TNF.

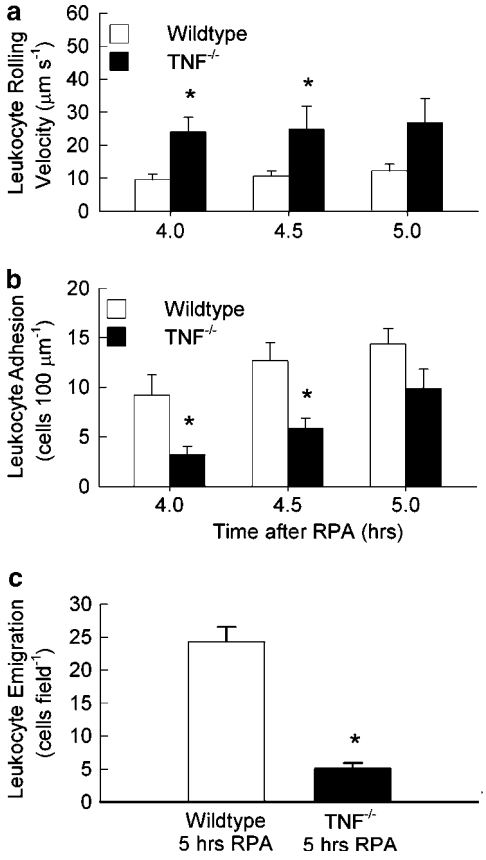

Figure 2 Leukocyte rolling velocity (a), adhesion (b) and emigration (c) in cremasteric postcapillary venules of wild-type and TNF$^{-/-}$ mice, 4–5 h after induction of the RPA response. Data are shown as mean ± s.e.m. of six animals. *Represents $P<0.05$ relative to RPA-treated wild-type mice.

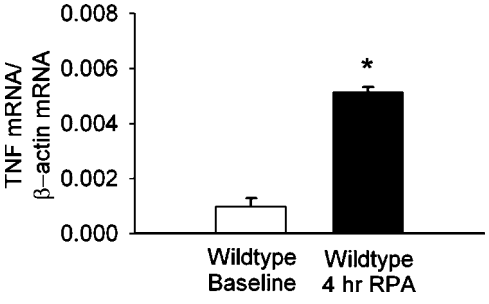

Figure 3 Quantification of TNF mRNA in wild-type mice using real-time PCR. Data are shown as mean ± s.e.m. of four animals. *Represents $P<0.05$ relative to untreated wild-type mice.

Given that previous studies have demonstrated a role for E-selectin in mediating rolling at slower velocities, the elevated leukocyte rolling velocity observed in TNF$^{-/-}$ mice during the RPA response (Figure 2a) is an additional finding, which is suggestive of the reduced involvement of E-selectin in TNF$^{-/-}$ mice (Kunkel & Ley, 1996; Hickey *et al*., 1998; Norman *et al*., 2003). To clarify the role of E-selectin in the RPA response in wild-type mice, we examined the effect of acute E-selectin blockade on leukocyte rolling velocity in wild-type mice. Administration of RME-1 in RPA-treated wild-type mice did not alter leukocyte rolling velocity (Figure 5a). Furthermore,

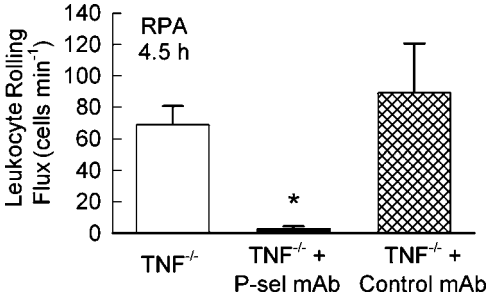

Figure 4 P-selectin blockade during the RPA response almost eliminates rolling in TNF$^{-/-}$ mice. P-selectin antibody was administered 4.25 h after RPA induction and rolling measured at 4.5 h post-RPA. Data represents mean ± s.e.m. of six animals. Also shown are RPA-treated TNF$^{-/-}$ mice treated with an isotype control antibody ($n=2$). *Denotes $P<0.05$ vs TNF$^{-/-}$ mice before anti-P-selectin treatment.

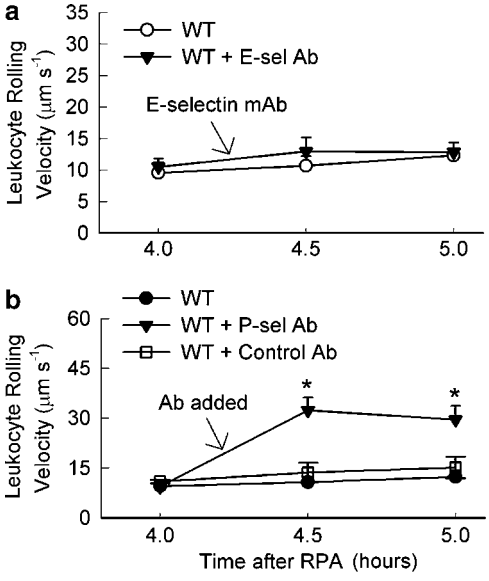

Figure 5 Effect of acute blockade of E-selectin (a) or P-selectin (b) on leukocyte rolling velocity in cremasteric postcapillary venules in RPA-treated wild-type (WT) mice. Separate groups of mice were treated with antibody 4.25 h post-RPA induction. Shown are untreated ($n=6$), anti-selectin antibody-treated mice ($n=6$) and in Panel B, mice treated with an isotype control antibody ($n=3$). Data represents mean ± s.e.m. *Denotes $P<0.01$ relative to RPA-treated wild-type mice.

the residual rolling after P-selectin blockade in wild-type mice, shown previously to be E-selectin-dependent, occurred at a significantly elevated velocity, an effect not seen after treatment with isotype control antibody (Figure 5b). These findings indicate that in this model of immune complex-induced inflammation, P-selectin, but not E-selectin, is primarily responsible for the reduction in leukocyte rolling velocity. This observation may be explained in part by our previous findings in this RPA model in which E-selectin expression is detectable in many fewer vessels than P-selectin (Norman *et al*., 2003).

Adhesion molecule expression in TNF$^{-/-}$ mice

The alterations in leukocyte rolling velocity and adhesion in the TNF$^{-/-}$ mice during the RPA response were suggestive of

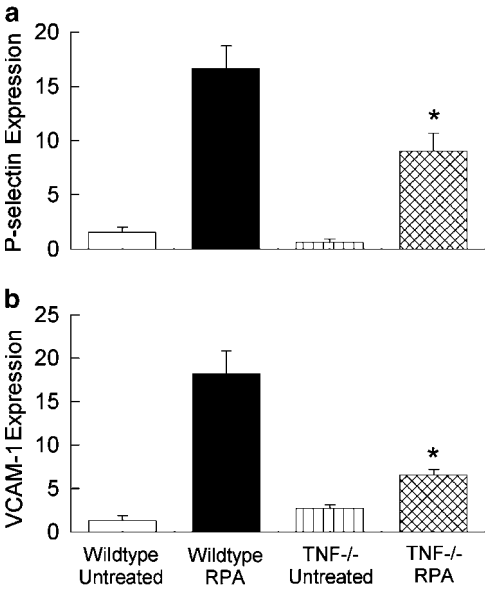

Figure 6 Expression of P-selectin (a) and VCAM-1 (b) in postcapillary venules in cremaster muscles from wild-type and TNF$^{-/-}$ mice, under baseline (untreated) conditions, and following RPA treatment (4 h). Data are expressed as the mean fluorescence intensity multiplied by the average length of positive vessels per field, and shown as mean ± s.e.m. For untreated mice, $n=2$ for P-selectin and VCAM-1. For RPA-treated wild-type and TNF$^{-/-}$ mice, $n=5$ for P-selectin, and $n=4$ for VCAM-1. *Denotes $P<0.05$ vs wild-type RPA.

changes in adhesion molecule expression. Therefore, we compared P-selectin expression in wild-type and TNF$^{-/-}$ mice 4 h after initiation of the RPA response (Figure 6). As seen previously (Norman *et al*., 2003), P-selectin is expressed at low levels in untreated wild-type animals, whereas 4 h after RPA-induction, P-selectin expression is markedly increased. In untreated TNF$^{-/-}$ mice as in wild-type mice, P-selectin expression is detectable at low levels. However, the level of P-selectin expression in RPA-treated TNF$^{-/-}$ mice is significantly lower than that in comparably treated wild-type mice (Figure 6a), increasing approximately 15 arbitrary units from basal levels vs an increase of only 8 units in TNF$^{-/-}$ mice.

We next examined the effect of RPA treatment on VCAM-1 expression. In contrast to P-selectin, which is expressed exclusively in postcapillary venules, VCAM-1 was also detectable in arterioles and capillaries (Figure 7). In both wild-type and TNF$^{-/-}$ mice, VCAM-1 expression was detectable at low levels in the uninflamed cremasteric microvasculature (Figure 6b). After the RPA response, VCAM-1 expression in RPA-treated wild-type mice was dramatically increased over baseline levels. This was seen both as an increase in the intensity of VCAM-1 staining in individual vessels, as well as an increase in the number of venules expressing VCAM-1 at detectable levels. In comparison, VCAM-1 staining in the RPA-treated TNF$^{-/-}$ mice was decreased significantly relative to that in wild-type mice.

Exogenous TNF rapidly increases adhesion in TNF$^{-/-}$ mice

In addition to an alteration in rolling velocity, we also observed a reduction in leukocyte adhesion in TNF$^{-/-}$ mice.

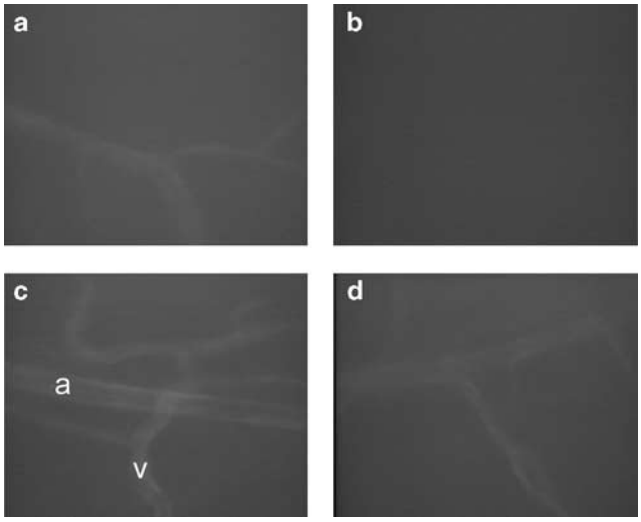

Figure 7 Effect of RPA treatment on anti-VCAM-1$^{ALEXA\ 488}$ staining in the murine cremasteric microvasculature. (a) VCAM-1 expression in an untreated wild-type mouse. (b) Effective exsanguination of the same field is demonstrated by illumination with appropriate wavelength fluorescence for the Alexa-594-conjugated control antibody. (c) Increased VCAM-1 staining is detectable in a wild-type mouse 4 h after RPA induction. Staining is present in a venule (v) and arteriole (a). (d) VCAM-1 staining in a TNF$^{-/-}$ mouse 4 h after RPA induction.

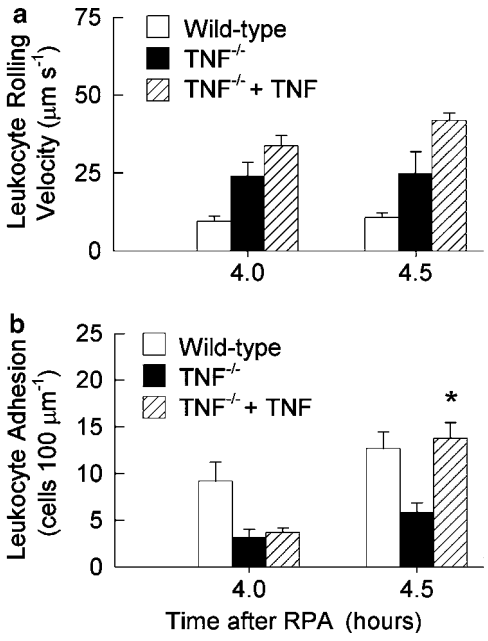

Figure 8 Effect of acute TNF superfusion (165 ng ml^{-1}) on leukocyte rolling velocity (a) and leukocyte adhesion (b) in RPA-treated TNF$^{-/-}$ mice ($n=5$). An initial measurement of rolling and adhesion was made immediately prior to 4 h. Then TNF was superfused over the preparation for 30 min commencing at 4 h, and leukocyte parameters were reevaluated 4.5 h post-RPA induction. Also shown are RPA-treated wild-type ($n=6$) and TNF$^{-/-}$ mice ($n=6$) in the absence of exogenous TNF. *Denotes $P<0.05$ vs untreated TNF$^{-/-}$ mice 4 h post-RPA induction.

This may have been directly related to the absence of the very slow rolling seen in the wild-type RPA-treated mice, as it has been observed previously that leukocyte adhesion occurs more readily at lower rolling velocities (Kanwar *et al*., 1995; Jung *et al*., 1998). However, it is also possible that the process of adhesion is directly regulated by TNF in the RPA model. To assess this possibility, TNF was applied acutely to TNF$^{-/-}$ mice after allowing 4 h for the typical development of the RPA response in the absence of TNF. Superfusion of the cremaster muscles of TNF$^{-/-}$ mice with TNF from 4 to 4.5 h rapidly restored adhesion to levels comparable to that seen in RPA-treated wild-type mice, without affecting leukocyte rolling flux (data not shown) or velocity (Figure 8). In fact, an increase in adhesion was already evident within 15 min of commencement of the TNF treatment. This suggests that TNF can modulate adhesion independently of its effect on leukocyte rolling parameters.

TNF mediates increased microvascular permeability in the RPA response

TNF has previously been observed to have differential roles in promoting immune complex-induced microvascular dysfunction in lung and skin (Mulligan & Ward, 1992). To evaluate the role of TNF in the muscle microvasculature, we assessed microvascular permeability during the RPA response. Figure 9 shows that 4.5 h after initiation of the RPA response in wild-type mice, leakage of FITC-dextran from cremasteric microvessels was significantly elevated above that in both untreated wild-type mice and in wild-type mice treated with OVA and rabbit IgG. In contrast, microvascular leakage in RPA-treated TNF$^{-/-}$ mice was not different to that in untreated TNF$^{-/-}$ mice. Furthermore, the level of microvascular leakage in untreated animals did not differ between the strains. As further

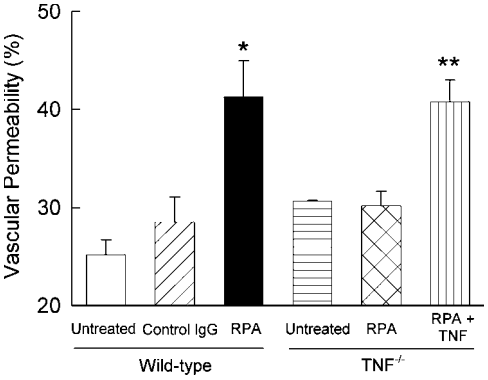

Figure 9 Alterations in microvascular permeability induced by the RPA response in wild-type and TNF$^{-/-}$ mice. Permeability in cremasteric postcapillary venules was assessed in untreated mice, and 4.5 h after initiation of the RPA response. Shown are untreated wild-type mice, wild-type mice treated with OVA and control IgG, RPA-treated wild-type mice (OVA and anti-OVA), untreated TNF$^{-/-}$ mice, RPA-treated TNF$^{-/-}$ mice, and RPA-treated TNF$^{-/-}$ mice treated with exogenous TNF (50 ng) at the initiation of the response ($n=6$ in each group, except untreated TNF$^{-/-}$ where $n=2$, and TNF$^{-/-}$ + exogenous TNF where $n=3$). *Denotes $P<0.05$ of wild-type RPA mice relative to all other groups, except TNF$^{-/-}$ + exogenous TNF. **Denotes $P<0.05$ vs RPA-treated TNF$^{-/-}$ mice.

assessment of the role of TNF in promoting increased vascular permeability, we also examined TNF$^{-/-}$ mice treated with local TNF (50 ng, intrascrotal) at the start of the RPA response. This treatment restored leukocyte adhesion to levels

seen in RPA-treated wild-type mice (data not shown). Furthermore, the level of vascular permeability in these animals was indistinguishable from that in wild-type RPA-treated mice (Figure 9). Together these experiments indicate that TNF plays a key role in promoting immune complex-induced alterations in microvascular permeability in the muscle microvasculature.

Discussion

TNF has been implicated as having a key role in the development of inflammation in immune complex-mediated responses (Warren *et al*., 1989; Warren, 1991; Mulligan & Ward, 1992; Mulligan *et al*., 1993; Brito *et al*., 1999). However, the direct influence of this cytokine on leukocyte–endothelial cell interactions in immune complex-mediated inflammation has not been examined. The data presented in this study reveal an important role for TNF in mediating the individual steps of the leukocyte recruitment cascade in the RPA response. The absence of TNF during the RPA response resulted in increased leukocyte rolling velocity, and reduced adhesion and emigration compared to wild-type animals. The alterations in rolling in the $TNF^{-/-}$ mice were due to the reduced expression of P-selectin, as well as the absence of functional E-selectin. While it is conceivable that the additional reductions in adhesion and emigration resulted directly from alterations in rolling, two pieces of evidence suggested that TNF also directly affects adhesion. Firstly, expression of VCAM-1, which we have previously observed to be of key importance in RPA-induced adhesion, was reduced in RPA-treated $TNF^{-/-}$ mice. Secondly, treatment of $TNF^{-/-}$ mice with exogenous TNF was able to reconstitute adhesion rapidly to levels seen in wild-type mice, without altering rolling parameters. These findings are the first demonstration of the key role of TNF in promoting both rolling and adhesion in the RPA response.

Previous experiments have shown that both P- and E-selectin play a role in leukocyte rolling in the RPA response in cremasteric postcapillary venules (Norman *et al*., 2003). The present studies demonstrate that TNF is responsible for the expression of E-selectin at functional levels, in addition to promoting increased expression of P-selectin. The observation that leukocyte rolling velocity is elevated in the absence of TNF indicates that these TNF-mediated increases in selectin expression are responsible for the markedly reduced rolling velocity observed in wild-type mice. We initially hypothesized that the increased leukocyte rolling velocity in TNF-deficient mice could be explained solely by the absence of functional E-selectin. Previous studies have shown that application of TNF to the cremaster muscle causes an E-selectin-dependent reduction in rolling velocity (Kunkel & Ley, 1996). However, in the RPA model, blockade of E-selectin function did not alter leukocyte rolling velocity. In contrast, blockade of P-selectin resulted in a significant increase in leukocyte rolling velocity. These findings indicate that in this model P-selectin, but not E-selectin, is of key importance in mediating the slow rolling observed. This may, in part, be due to the differences in the relative levels of expression of the two endothelial selectins during the RPA response. *Via* direct visualization of selectin expression in the cremaster muscle, we have previously observed that at the peak of E-selectin expression (2.5–4 h), E-selectin is detectable in less than 50% of the venules in which P-selectin is observed (Norman *et al*., 2003). It is probable that the minimal role of E-selectin in reducing rolling velocity in the present experiments is due to its less extensive level of expression relative to other models of inflammation (Kunkel & Ley, 1996; Jung *et al*., 1998).

In addition to its effects on rolling, the absence of TNF also resulted in a significant reduction in leukocyte adhesion induced by the RPA reaction. There are a number of potential reasons for this response. It may be a result of the increase in leukocyte rolling velocity in $TNF^{-/-}$ mice, as it has been shown that leukocyte adhesion is more likely to occur at slow leukocyte rolling velocities (Jung *et al*., 1998). The observed reduction in VCAM-1 expression in $TNF^{-/-}$ mice raises an alternative explanation. Previously, we have shown that VCAM-1 plays a key role in leukocyte adhesion and emigration in the RPA response in the cremaster muscle (Norman *et al*., 2003). Therefore, a reduction in VCAM-1 expression in $TNF^{-/-}$ mice would be expected to result in a comparable reduction in leukocyte adhesion.

Alternatively, the current data also raise the possibility that in immune complex-induced responses, TNF can induce adhesion within minutes of its release. This is supported by our observation that the reduced leukocyte adhesion in the RPA-treated $TNF^{-/-}$ mouse could be restored to that seen in wild-type animals by 30 min of acute application of TNF to the cremasteric microvasculature, in the absence of alterations in rolling parameters. Similar observations of a rapid increase in leukocyte adhesion in response to short-term application of TNF have been reported previously (Thorlacius *et al*., 2000; Young *et al*., 2002). Thorlacius *et al*. showed that 30 min exposure of the cremaster muscle to TNF was sufficient to induce a marked increase in leukocyte adhesion without altering leukocyte rolling parameters. Moreover, Young *et al*. (2002) have recently reported that the rapid increase in adhesion induced by TNF is unaffected by inhibition of protein synthesis *via* actinomycin D. These findings indicate that the rapid adhesive response induced by TNF does not require *de novo* synthesis of adhesion molecules, but presumably involves molecules already expressed by leukocytes and endothelial cells. In support of this contention, exposure of murine neutrophils to TNF *in vitro* has been shown to induce a rapid increase in β_2 integrin expression, suggesting that the leukocyte maybe a potential target of TNF in this system (Young *et al*., 2002). Alternatively, it is conceivable that TNF can promote rapid changes in avidity of endothelial adhesion molecules, thereby promoting leukocyte arrest on the endothelial surface. Indeed, TNF has recently been shown to promote phosphorylation of ICAM-1 in endothelial cells within 1 min, at the same time as causing a 10-fold increase in adhesivity for neutrophils (Javaid *et al*., 2003).

In addition to reducing leukocyte recruitment, the absence of TNF was associated with a significant reduction in the immune complex-induced alteration in microvascular permeability, suggesting that TNF-mediated leukocyte recruitment plays a key role in injuring the vasculature and promoting microvascular leakage. This is supported by observations of immune complex-induced injury in the lung in which prevention of leukocyte recruitment *via* blockade of key adhesion molecule pathways protects against microvascular injury (Mulligan *et al*., 1991). Interestingly, TNF does not have the same role in all tissues. While anti-TNF treatment reduces both leukocyte recruitment and microvascular injury in the

lung, in the skin the same treatment is without effect on either recruitment or permeability (Warren *et al*., 1989; Mulligan & Ward, 1992). The basis of the tissue specificity of this response is unclear. However, taken together with the present data, these findings indicate that the effectiveness of TNF at inducing leukocyte recruitment in response to immune complex formation varies according to the vascular bed. Furthermore, anti-TNF therapy is effective at reducing microvascular injury only in tissues in which TNF promotes recruitment. This consistent correlation of recruitment and microvascular injury strongly suggests that the effect of TNF on microvascular permeability in immune complex-induced inflammation is due to its ability to promote leukocyte recruitment.

We have previously demonstrated in this RPA model that immune complexes initially form in the perivascular tissue when OVA leaves the vasculature, and that microvascular permeability increases rapidly in response to this initial immune complex formation. Given the increased leakage in wild-type vs $TNF^{-/-}$ mice, it is conceivable that an additional effect of the microvascular leakage induced by TNF may be to allow a greater level of immune complex formation. Previous work has shown that the level of the inflammatory response is determined by the amount of immune complex formation (Mulligan & Ward, 1992). Therefore, increased complex formation afforded by an increase in macromolecular leakage into the interstitium would be expected to result in an amplification of the inflammatory response. This may represent an additional pathway whereby TNF promotes immune complex-induced inflammation in the cremasteric microvasculature.

Together these observations indicate that the actions of cytokines such as TNF during inflammatory responses are remarkably diverse, potentially having both immediate and long-term effects, and targeting multiple physiological processes including rolling, adhesion and macromolecular leakage. Furthermore, these data demonstrate that experiments in which production/release of a cytokine is stimulated as part of an inflammatory response can provide divergent data relative to studies in which cytokines are applied directly to tissues.

This work was supported by a project grant from the National Health & Medical Research Council (NHMRC) of Australia (#236910). M. Hickey is an NHMRC R.D. Wright Fellow. M.U. Norman is an NHMRC C.J. Martin Postdoctoral Fellow.The authors thank Drs Jonathan Sedgwick and Nick Pearce (Centenary Institute, Sydney, Australia) for the generous donation of the $TNF^{-/-}$ mice, and Drs Dietmar Vestweber and Britta Engelhardt (Max Planck Institut, Meunster, Germany), for their generous assistance in provision of the 6C7.1 hybridoma.

References

ABBASSI, O., KISHIMOTO, T.K., MCINTIRE, L.V., ANDERSON, D.C. & SMITH, C.W. (1993). E-selectin supports neutrophil rolling *in vitro* under conditions of flow. *J. Clin. Invest.*, **92,** 2719–2730.

BRITO, B.E., O'ROURKE, L.M., PAN, Y., ANGLIN, J., PLANCK, S.R. & ROSENBAUM, J.T. (1999). IL-1 and TNF receptor-deficient mice show decreased inflammation in an immune complex model of uveitis. *Invest. Ophthalmol. Vis. Sci.,* **40,** 2583–2589.

DRUMMOND, A.E., DYSON, M., THEAN, E., GROOME, N.P., ROBERTSON, D.M. & FINDLAY, J.K. (2000). Temporal and hormonal regulation of inhibin protein and subunit mRNA expression by post-natal and immature rat ovaries. *J. Endocrinol.,* **166,** 339–354.

FIRESTEIN, G.S. (2003). Evolving concepts of rheumatoid arthritis. *Nature,* **423,** 356–361.

HENNINGER, D.D., PANES, J., EPPIHIMER, M.J., RUSSELL, J., GERRITSEN, M.E., ANDERSON, D.C. & GRANGER, D.N. (1997). Cytokine-induced VCAM-1 and ICAM-1 expression in different organs of the mouse. *J.Immunol.,* **158,** 1825–1832.

HICKEY, M.J., ISSEKUTZ, A.C., REINHARDT, P.H., FEDORAK, R.N. & KUBES, P. (1998). Endogenous interleukin-10 regulates hemodynamic parameters, leukocyte–endothelial cell interactions, and microvascular permeability during endotoxemia. *Circ. Res.,* **83,** 1124–1131.

HICKEY, M.J., REINHARDT, P.H., OSTROVSKY, L., JONES, W.M., JUTILA, M.A., PAYNE, D., ELLIOT, J. & KUBES, P. (1997). Tumor necrosis factor-α induces leukocyte recruitment by different mechanisms *in vivo* and *in vitro*. *J. Immunol.,* **158,** 3391–3400.

JAVAID, K., RAHMAN, A., ANWAR, K.N., FREY, R.S., MINSHALL, R.D. & MALIK, A.B. (2003). Tumor necrosis factor-alpha induces early-onset endothelial adhesivity by protein kinase Czeta-dependent activation of intercellular adhesion molecule-1. *Circ. Res.,* **92,** 1089–1097.

JUNG, U. & LEY, K. (1997). Regulation of E-selectin, P-selectin, and intercellular adhesion molecule 1 expression in mouse cremaster muscle vasculature. *Microcirculation,* **4,** 311–319.

JUNG, U., NORMAN, K.E., SCHARFFETTER-KOCHANEK, K., BEAUDET, A.L. & LEY, K. (1998). Transit time of leukocytes rolling through venules controls cytokine-induced inflammatory cell recruitment *in vivo*. *J. Clin. Invest.,* **102,** 1526–1533.

KANWAR, S., JOHNSTON, B. & KUBES, P. (1995). Leukotriene C4/D4 induces P-selectin and sialyl Lewis(x)-dependent alterations in leukocyte kinetics *in vivo*. *Circ. Res.,* **77,** 879–887.

KORNER, H., COOK, M., RIMINTON, D.S., LEMCKERT, F.A., HOEK, R.M., LEDERMANN, B., KONTGEN, F., FAZEKAS DE ST GROTH, B. & SEDGWICK, J.D. (1997). Distinct roles for lymphotoxin-alpha and tumor necrosis factor in organogenesis and spatial organization of lymphoid tissue. *Eur. J. Immunol.,* **27,** 2600–2609.

KUNKEL, E.J. & LEY, K. (1996). Distinct phenotype of E-selectin-deficient mice. E-selectin is required for slow leukocyte rolling *in vivo*. *Circ. Res.,* **79,** 1196–1204.

LUSCINSKAS, F.W., DING, H. & LICHTMAN, A.H. (1995). P-selectin and vascular cell adhesion molecule 1 mediate rolling and arrest, respectively, of CD4+ T lymphocytes on tumor necrosis factor alpha-activated vascular endothelium under flow. *J. Exp. Med.,* **181,** 1179–1186.

MCCAFFERTY, D.M., KANWAR, S., GRANGER, D.N. & KUBES, P. (2000). E/P-selectin-deficient mice: an optimal mutation for abrogating antigen but not tumor necrosis factor-alpha-induced immune responses. *Eur. J. Immunol.,* **30,** 2362–2371.

MOK, C.C. & LAU, C.S. (2003). Pathogenesis of systemic lupus erythematosus. *J. Clin. Pathol.,* **56,** 481–490.

MULLER, W.A. (2002). Leukocyte–endothelial cell interactions in the inflammatory response. *Lab. Invest.,* **82,** 521–533.

MULLIGAN, M.S. & WARD, P.A. (1992). Immune complex-induced lung and dermal vascular injury. Differing requirements for tumor necrosis factor-alpha and IL-1. *J. Immunol.,* **149,** 331–339.

MULLIGAN, M.S., VAPORCIYAN, A.A., MIYASAKA, M., TAMATANI, T. & WARD, P.A. (1993). Tumor necrosis factor alpha regulates *in vivo* intrapulmonary expression of ICAM-1. *Am. J. Pathol.,* **142,** 1739–1749.

MULLIGAN, M.S., VARANI, J., DAME, M.K., LANE, C.L., SMITH, C.W., ANDERSON, D.C. & WARD, P.A. (1991). Role of endothelial-leukocyte adhesion molecule 1 (ELAM-1) in neutrophil-mediated lung injury in rats. *J. Clin. Invest.,* **88,** 1396–1406.

NORMAN, M.U., VAN DE VELDE, N.C., TIMOSHANKO, J.R., ISSEKUTZ, A. & HICKEY, M.J. (2003). Overlapping roles of endothelial selectins and vascular cell adhesion molecule-1 in immune complex-induced leukocyte recruitment in the cremasteric microvasculature. *Am. J. Pathol.,* **163,** 1491–1503.

SPRINGER, T.A. (1994). Traffic signals for lymphocyte recirculation and leukocyte emigration: the multistep paradigm. *Cell,* **76,** 301–314.

THOMPSON, R.D., NOBLE, K.E., LARBI, K.Y., DEWAR, A., DUNCAN, G.S., MAK, T.W. & NOURSHARGH, S. (2001). Platelet-endothelial cell adhesion molecule-1 (PECAM-1)-deficient mice demonstrate a transient and cytokine-specific role for PECAM-1 in leukocyte migration through the perivascular basement membrane. *Blood,* **97,** 1854–1860.

THORLACIUS, H., VOLLMAR, B., GUO, Y., MAK, T.W., PFREUNDSCHUH, M.M., MENGER, M.D. & SCHMITS, R. (2000). Lymphocyte function antigen 1 (LFA-1) mediates early tumour necrosis factor alpha-induced leucocyte adhesion in venules. *Br. J. Haematol.,* **110,** 424–429.

WARREN, J.S. (1991). Disparate roles for TNF in the pathogenesis of acute immune complex alveolitis and dermal vasculitis. *Clin. Immunol. Immunopathol.,* **61,** 249–259.

WARREN, J.S., YABROFF, K.R., REMICK, D.G., KUNKEL, S.L., CHENSUE, S.W., KUNKEL, R.G., JOHNSON, K.J. & WARD, P.A. (1989). Tumor necrosis factor participates in the pathogenesis of acute immune complex alveolitis in the rat. *J. Clin. Invest.,* **84,** 1873–1882.

YOUNG, R.E., THOMPSON, R.D. & NOURSHARGH, S. (2002). Divergent mechanisms of action of the inflammatory cytokines interleukin 1-beta and tumour necrosis factor-alpha in mouse cremasteric venules. *Br. J. Pharmacol.,* **137,** 1237–1246.

(Received August 13, 2004
Revised October 22, 2004
Accepted November 2, 2004)